

## Design of Optimal Sliding Mode Control of Elbow Wearable Exoskeleton System Based on Whale Optimization Algorithm



Zharaa A. Waheed, Amjad J. Humaidi\*

Control and Systems Engineering Department, University of Technology-Iraq, Baghdad 10066, Iraq

Corresponding Author Email: [amjad.j.humaidi@uotechnology.edu.iq](mailto:amjad.j.humaidi@uotechnology.edu.iq)

<https://doi.org/10.18280/jesa.550404>

### ABSTRACT

**Received:** 14 July 2022

**Accepted:** 20 August 2022

**Keywords:**

*exoskeleton system, exoskeleton system for rehabilitation, sliding mode control*

The high nonlinearity and time-varying coefficients characterize the elbow exoskeleton system for rehabilitation. To deal with these difficult control challenges, nonlinear and reliable controllers are needed. This paper shows the use of Sliding Mode Control (SMC) to track the trajectory of an Elbow Exoskeleton System (EES) with presence of parameter uncertainty. The Whale Optimization Algorithm (WOA) algorithm is used to tuning the design parameters of suggested controllers for performance improvement. Computer simulation based on MATLAB software has been implemented to conduct a comparison study between optimal and non-optimal SMC. The simulation findings shows that the optimal SMC outperforms the non-optimal version of controller in terms of performance.

## 1. INTRODUCTION

Due to a variety of circumstances, joint dysfunction disables a vast number of people each year. Control ability of muscle manifests itself in these people as torque production and a failure to modulate mechanical impedance around the joints. Therefore, the rehabilitation procedures can be utilized by many of these disable patients to help them in restoring their health and returning to their regular life [1-5]. The accidents and pathology are the main cause of elbow disabilities in human being. In any of these circumstances, the resulting consequence leads to injury of muscles or nerve. This in turn leads to faults in motor functions and finally to paralysis. To provide a solution to problems in weakness of muscle and nerve, the assistive and rehabilitation equipment and tools came out to help the mobility of disabled individuals with various disabilities. In the Neuro-rehabilitation process, the programs are gradually been incorporated with aid of robotic devices [6].

Exoskeletons are wearable robots which are fit and interact with patient on a cognitive and physical system. These robotic exoskeleton systems work in conjunction with human limbs. Researches and developments of Exoskeleton devices have started in the early 1960s; however, they have been only recently applied in patients with motor deficits for functional replacement and rehabilitation. These exoskeleton devices are articulated mechanical systems which are supplied by sensors and actuators to achieve their functions properly. According to the size and weight of disables parts of human being, the type of actuators is dedicated that can achieve the stroke and force requirements of worn exoskeletal/orthotic system. In addition, the number of actuators depend on the number of joints to be exercised. In addition, the challenges of computation and control design are based on the number of degrees of freedoms (DoF) which are possessed by human musculoskeletal systems. As a result, if an efficient design is to be achieved, the control system is important. In order for the

system to work properly, it needs to take into account factors like how quickly and where each limb moves, how well it can adapt to its environment, and how much energy each limb needs. These are all factors that must be taken into account [6-8].

In practice, the exoskeleton device will replace the physician specialist who is responsible for movement of disabled parts for rehabilitation of these members. However, to make this device be universal for any individual and to take into account the variations in system parameters due to human coupling, the need of robust control is an essential to develop successful control model for exoskeleton systems. In this study, control strategy have been used for elbow exoskeleton system, namely: SMC. It has been shown that the sliding mode control technique is efficient in control of complex and higher order nonlinear systems in the presence of uncertainties. In the literature, one can find the utilization of SMC in many control applications [9-16].

In this study, sliding mode controller has been developed and optimized based on whale optimization algorithm for motion control of elbow joint utilizing wearable exoskeleton rehabilitation system. The main contributions of this study can be highlighted by the following points:

- (1) Developing the control laws based of SMC to guide the error trajectories from initial conditions to the zero equilibrium points in finite time.
- (2) Developing the optimization algorithm based on WOA for tuning the design parameters of elbow exoskeleton system to enhance the dynamic performance of controlled system.

The article has been organized as follows: Section 2 presents the various control schemes for controlling the elbow joint. Section 3 analyzed the dynamic model of the elbow motion. In Section 4, the control design methodology has been presented and analyzed. Section 5 developed the optimization algorithm based on WOA. The numerical simulation has been presented in Section 6, while the Section 7 highlighted the main concluded points of this study.

## 2. RELATED WORKS

In what follows, a brief explanation of different control researches which addressing the motion control of human upper-limb are presented:

Barbouch et al. [17] have investigated the performance and robustness of a Feedback Error learning scheme mixed with sliding mode control (SMC) to motion control of elbow joint based on Functional Electrical Stimulation system. Babaiasl et al. [18] presented new mechanical design of 3 DoF exoskeleton robot for rehabilitation of shoulder joint. The study proposed SMC to track desired trajectories and the genetic algorithm has been applied for optimal tuning of design parameters of proposed controller. Nguyen et al. [19] developed adaptive intelligent controller which combines both fuzzy logic (FL) technique and PID control for upper-limb exoskeleton robot actuated by pneumatic artificial muscle. The PID controller is used to compensate the approximating error and hysteresis characteristics, while the FL part is responsible for estimating the nonlinear functions. Hu et al. [20] have developed an assist-as-needed control algorithm for flexible exoskeletons applied for rehabilitation of upper-limb part of disabled patients. The elbow exoskeleton is mechanically designed to be driven by flexible antagonistic cable actuators. Brahim et al. [21] have presented backstepping sliding mode control design for pre-described path tracking of ETS-MARSE exoskeleton robot applied for passive rehabilitation exercises. The robot is worn by persons at the upper limb to help treatment of impaired upper limb functions due to stroke. Liu et al. [22] have established adaptive fuzzy neural network (AFNN) for estimating the angle of elbow joint based on surface electromyography (sEMG). The AFNN showed better accuracy and rapidity as compared with other neural network structures, back-propagation-based NN and Radial basis-based NN. Yang et al. [23] developed model free backstepping sliding mode control strategy for wearable exoskeletons. The non-singular fast terminal sliding controller is combined with auxiliary backstepping controller to improve the control performance. The lumped uncertainties are estimated via time-delay estimation. Bembli et al. [24] presented robust adaptive sliding mode algorithm based on gravity compensation to control the upper limb exoskeleton system subjected to parametric uncertainties. The rehabilitation system is two degrees of freedom robot to achieve movement of the elbow and shoulder joints. Islam et al. [25] proposed fractional sliding mode control (FSMC) to control 7 DOF u-Rob (upper limb robotic exoskeleton) subjected to unmodeled dynamics. As compared to classical sliding mode control (SMC), the FSMC showed better performance in terms of tracking and chattering effect in control signal.

It has been shown that the design parameters of proposed controllers have a direct impact of their performances. The conventional way to set these design parameters is based on try-and-error procedure. However, this classical setting of parameters does not yield optimal performance of controllers, as such modern optimization technique has to be used for optimal tuning of these parameters. Based on the above literature review, the previous control approaches did not address the effect of design parameters on the dynamic performance of controlled system.

This gap of optimal tuning has been filled by this study and the tuning of these design has been implemented using WOA. This optimization techniques will lead to optimal performance of controllers and consequently the optimal performance of controlled exoskeleton elbow-system.

## 3. MODELLING OF ELBOW ASSISTIVE SYSTEM

Figure 1 represents the exoskeleton device attached to the elbow. The device is used to assist motion of patient joint using actuator [25].

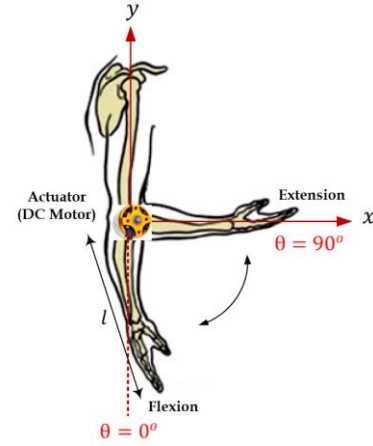


**Figure 1.** Schematic representation of elbow flexion and extension movements [25]

The dynamic model of both the human arm and exoskeleton are derived simultaneously. The Euler-Lagrange equation is firstly established based on the following [26]:

$$L_i = E_{ki} - E_{gi} \quad (1)$$

$$\frac{d}{dt} \frac{\partial L}{\partial \dot{\theta}} - \frac{\partial L}{\partial \theta} = \tau \quad (2)$$

where,  $E_{ki}$  and  $E_{gi}$  are represented by the kinetic and gravitational energies of the system and it is given by:

$$E_{ki} = \frac{1}{2} I_i \dot{\theta}^2 \quad (3)$$

$$E_{gi} = g m_i l_i (1 - \cos \theta) \quad (4)$$

where,  $I_i$  is the inertia of the human elbow and exoskeleton and  $i \in (1,2)$ ,  $m_i$ ,  $g$  and  $l_i$  represent the mass of the human elbow and exoskeleton, the acceleration due to gravity, and the distance between the elbow joint and center of gravity, respectively [26].

$$I_i = \frac{1}{2} m_i l_i^2 \quad (5)$$

Substitution Eq. (3) and Eq. (4) into Eq. (1) gives:

$$L_i = \frac{1}{2} I_i \dot{\theta}^2 - g m_i l_i (1 - \cos \theta) \quad (6)$$

$$\tau_g = g m_i l_i \quad (7)$$

$$\tau_{exti} = \tau_{ki} + \tau_i \quad (8)$$

where,  $\tau_g$  and  $\tau_{exti}$  represent the system's gravitational torque and external torque acting on the system, and  $\tau_{fi}$  and  $\tau_i$  represent the friction and motor control torque respectively.

$$\tau_{ki} = K_v \dot{\theta} \quad (9)$$

where,  $k_v$  represent viscous friction coefficients.

On deriving Eq. (6), using the Euler-Lagrange equation the resulting dynamics of the system can be written as [26]:

$$\tau_e = I\ddot{\theta} + \tau_g \sin \theta \quad (10)$$

Let  $\tau_i = \tau_e$ , which is the single applied torque, then Eq. (11) becomes:

$$\tau_e = I\ddot{\theta} + \tau_g \sin \theta \quad (11)$$

The system model consists of the human leg and exoskeleton is given by:

$$I\ddot{\theta} = \tau_g \sin \theta + k_v \dot{\theta} + \tau_e \quad (12)$$

where,  $I = \sum_{i=1}^2 I_i$ ,  $F = \sum_{i=1}^2 F_i$ ,  $B = \sum_{i=1}^2 B_i$ ,  $\theta$ ,  $\dot{\theta}$ ,  $\ddot{\theta}$  represent the angular position, velocity, and acceleration of the coupled system respectively.

Eq. (12) can be written in a robotic form as follows:

$$M(\theta)\ddot{\theta} + f(\theta, \dot{\theta}) + G(\theta) = \tau_e \quad (13)$$

Hence, Eq. (13) can be written as:

$$\ddot{\theta} = M(\theta)^{-1} (\tau_e - f(\theta, \dot{\theta}) - G(\theta)) \quad (14)$$

Furthermore, Eq. (14) can be written in state variables as follows:

$$\dot{x}_1 = \dot{\theta} = x_2 \quad (15)$$

$$\dot{x}_2 = \ddot{\theta} = \frac{1}{I} (\tau_e - k_v(x_2) - \tau_g \sin(x_1)) \quad (16)$$

#### 4. DESIGN OF SMC FOR ELBOW EXOSKELETON SYSTEM

In this part, the control laws are developed based on SMC in the presence of uncertainty in system parameters. The sliding surface is synthesized to derive the control law based on controlled system [27, 28].

Assuming that  $e$  is the difference between the current position  $x_1 = \theta$  and the desired trajectory,  $x_{1d} = \theta_d$ .

$$e = x_1 - x_{1d} \quad (17)$$

Using Eq. (15) and Eq. (16), the first and second derivative is given by [29]:

$$\dot{e} = \dot{x}_1 - \dot{x}_{1d} = x_2 - \dot{x}_{1d} \quad (18)$$

$$\ddot{e} = \dot{x}_2 - \ddot{x}_{1d} \quad (19)$$

$$\ddot{e} = \frac{1}{I} ((\tau_e - K_v x_2 - \tau_g \sin(x_1))) - \ddot{x}_{1d} \quad (20)$$

where,  $\tau$  represent the applied torque or the actuating control signal. The sliding surface is chosen according the order of controlled system [30]:

$$s = c e + \dot{e} \quad (21)$$

Using Eq. (18) and Eq. (20), the first-time derivative of sliding surface equation is given by:

$$\dot{s} = c \dot{e} + \dot{x}_2 - \ddot{x}_{1d} \quad (22)$$

where,  $c$  is defined as scalar design parameter. According to Eq. (16), Eq. (22) becomes:

$$\dot{s} = c \dot{e} + \frac{1}{I} (\tau_e - K_v x_2 - \tau_g \sin(x_1)) - \ddot{x}_{1d} \quad (23)$$

Letting  $\tau_e = u$ , Eq. (23) can be written as:

$$\dot{s} = c \dot{e} + \frac{1}{I} (u - K_v x_2 - \tau_g \sin(x_1)) - \ddot{x}_{1d} \quad (24)$$

Based on SMC approach, the control law  $u$  is composed of:

$$u = u_{eq} + u_{sw} \quad (25)$$

where,  $u_{eq}$  is the equivalent part and  $u_{sw}$  represents the switching part; that is:

$$u_{eq} = I(K_v x_2 + \tau_g \sin(x_1)) - c \dot{e} + \ddot{x}_{1d} \quad (26)$$

$$u_{sw} = -\beta_1 \text{sign}(s) \quad (27)$$

where,  $\beta_1$  represents a scalar design constant. When setting sliding surface and its derivative to zero ( $s=0$ ,  $\dot{s}=0$ ), the control law  $u$  can be deduced.

$$u = I(K_v x_2 + \tau_g \sin(x_1)) - c \dot{e} + \ddot{x}_{1d} - \beta_1 \text{sign}(s) \quad (28)$$

#### 5. WHALE OPTIMIZATION ALGORITHM

Whale Optimization Algorithm (WOA) is a new search algorithm developed in recent years. It is based on the concept of whale social behaviour [31].

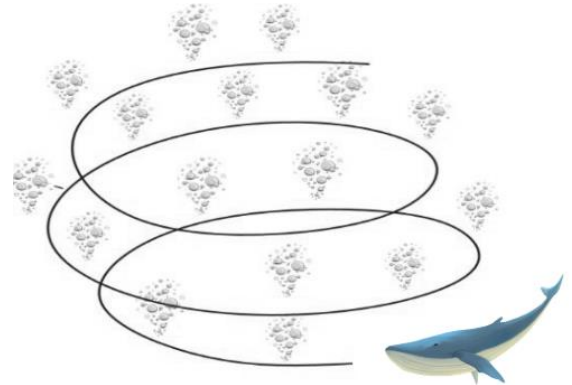


**Figure 2.** Bubble-net feeding behavior of humpback whales

The Humpback whales are the largest among all types of whales. Whales enjoy chasing krill and small fish. The humpback whale hunting method is based on bubble-net feeding. WOA numerically demonstrates the twisting bubble-net nourishing plan [32]. During the hunting process,

humpback whales exhibit some essential behaviours. This foraging is done by creating distinctive bubbles along a circle or '9'-shaped path as shown in Figure 2. The WOA can be splitted into sub-algorithms or steps. Each step is inspired from the behaviour of whale nature [33].

### 5.1 Encircling prey

The best ability of whales is how to identify the location of the prey and then begin surrounding it. Because the initial position of the prey is unknown, the WOA algorithm considers the present optimal solution to be close to the most possible solutions. After obtaining the current best position, the other search agents change their position toward that of the current best search agent. It can be expressed mathematically as:

$$\vec{D} = |\vec{C} \cdot \vec{X}(t) - \vec{X}^*(t)| \quad (29)$$

$$\vec{X}(t+1) = \vec{X}^*(t) - \vec{A} \cdot \vec{D} \quad (30)$$

$$\vec{A} = 2\vec{a} \vec{r} - \vec{A} \quad (31)$$

$$\vec{C} = 2 \vec{r} \quad (32)$$

where,  $\vec{X}^*$  is the general position vector,  $\vec{X}$  symbolize whale position,  $t$  specifies the current iteration,  $\vec{a}$  represents linearly reduced within the range of 2 to 0 throughout iterations, and  $r$  is a random number uniformly distributed in the range of [0, 1] [34].

### 5.2 Bubble-net attacking method (Exploration phase)

The humpback whale bubble-net behavior is explained in the following sections.

#### 5.2.1 Shrinking encircling mechanism

This behavior is achieved by decreasing the value of  $\vec{A}$ . Note that the fluctuation range of  $\vec{A}$  is also decreased by  $\vec{a}$ . Setting random values for  $\vec{A}$  in [-1, 1], the new position of a search agent can be defined anywhere between the original position of the agent and the position of the current best agent.

#### 5.2.2 Spiral updating position

This approach first calculates the distance between the whale located at (X, Y) and prey located at (X\*, Y\*). A spiral equation is then created between the position of whale and prey to mimic the helix-shaped movement of humpback whales as follows:

$$\vec{X}(t+1) = \vec{D}^i e^{bl} \cos(2\pi l) + \vec{X}^*(t) \quad (33)$$

where,  $\vec{D} = |\vec{X}^*(t) - \vec{X}(t)|$  and indicates the distance of the  $i$ -th whale to the prey (best solution obtained so far),  $b$  is a constant for defining the shape of the logarithmic spiral, and  $t$  is a random number in [-1, 1] [35].

It the worth mentioning that humpback whales swim around their prey in a shrinking circle while also following a spiral-shaped path. To model this simultaneous behavior, assume that there is a 50% chance of selecting either the shrinking encircling mechanism or the spiral model to update the position of whales during optimization. The following is the mathematical model:

$$\vec{X}(t+1) = \begin{cases} \vec{X}^*(t) - \vec{A} \cdot \vec{D} & p < 0.5 \\ \vec{D}^i e^{bl} \cos(2\pi l) + \vec{X}^*(t) & p \geq 0.5 \end{cases} \quad (34)$$

where,  $p$  is a random number in [0, 1].

### 5.3 Search for prey (Exploration phase)

The same approach based on the variation of the  $\vec{A}$  vector can be utilized to search for prey (exploration). In fact, humpback whales search randomly according to their position each other. Therefore, the  $\vec{A}$  with the random values greater than 1 or less than -1 to force the search agent to move far away from a reference whale. In contrast to the exploitation phase, whales update the position of a search agent in the exploration phase according to a randomly chosen search agent instead of the best search agent. This mechanism and  $|\vec{A}| > 1$  emphasize exploration and allows the WOA algorithm to perform a global search. The mathematical model is as follows:

$$\vec{D} = |\vec{C} \cdot \vec{X}(t) - \vec{X}(t)| \quad (35)$$

$$\vec{X}(t+1) = \vec{X}rand - \vec{A} \cdot \vec{D} \quad (36)$$

In this application, the parameters of WOA are set according to Table 1. The pseudo-code of the WOA algorithm is presented below:

```

Input data, Number of maxiter and Population, etc.
Initialize the whales population Xi (i=1, 2, ..., n)
Initialize a, A, C, l and p
Calculate the fitness of each search agent
X*=the best search agent
while (it<Maxiter)
for each search agent
if (p<0.5)
if (|A|<1)
Update the position of the current search agent by
Eq. (33)
else if (|A|≥1)
Select a random search agent (X_rand)
Update the position of the current search agent by Eq.
(34)
end
else if (p≥0.5)
Update the position of the current search agent by the Eq.
(36)
End

```

**Table 1.** Parameter setting of WOA

WOA Algorithm Parameters	Value
Random values	r1, r2
Population size	30
Iterations No.	300

Other optimization techniques like Butterfly Optimization Algorithm (BOA), Social Spider Optimization (SSO), Grey-Wolf Optimization (GWO), Spider Monkey Optimization (SMO), and Whale Optimization Algorithm (WOA) can be suggested for future tuning and optimization of proposed controller's design parameters in this application [36-40].

## 6. RESULT AND DISCUSSION

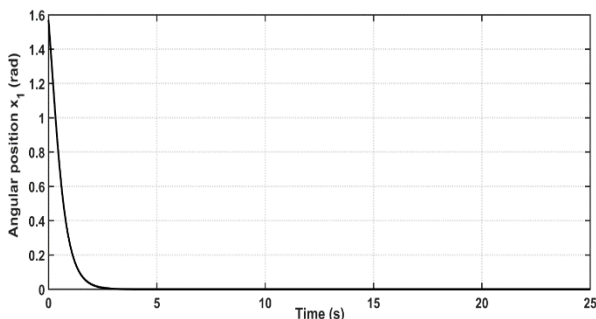
The programming simulation using MATLAB R2016 b, the simulation tests were performed on PC, Windows 10 OS, Intel(R) Core (TM) i7-8550 U processor, 1.80 GHz CPU, and 20 GB RAM. The Table 2 lists the numerical values for the Elbow-Exoskeleton system case. The simulation results were running for 3 seconds.

**Table 2.** Test model Specifications and test conditions

Coefficient Description	Value
Mass $M$	1.55 kg
Length $l$	0.24 m
Elbow joint to centre of gravity is $l_i$	0.2 m
Gravity acceleration $g$	9.81 m/s <sup>2</sup>
Viscous friction coefficients $k_v$	1.5 Nm/(rad/s)

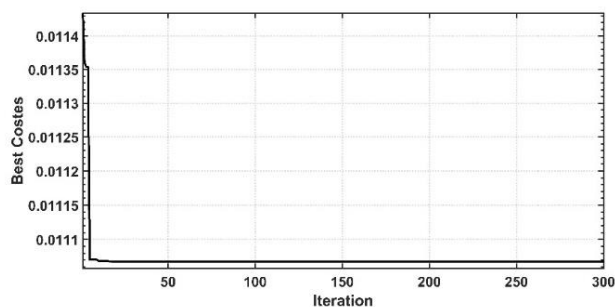
### 6.1 Simulation of elbow-exoskeleton system controlled by SMC

Figure 3 shows the open-loop test of Elbow-Exoskeleton system. The system is commanded by sine wave method. It is clear from the figure that the output response, represented by linear displacement  $x_1$ , has started from high position (1.6) rad, however, the response settles quickly just after around (2) seconds to reach nearly zero rad. The  $c$  and  $\beta_1$  are the design parameters of SMC, Increasing the dynamic performance of SMC by optimizing their design parameters is an objective of algorithm. As with other WOA processes, the iterative particles are evaluated using the RMSE fitness function.



**Figure 3.** Open loop response for the Elbow-Exoskeleton system

The goal of an optimization technique is to identify the best values for design parameters such that the RMSE is as low as possible. Figure 4 show the behaviour of the cost function for SMC.



**Figure 4.** Cost function for controlled system based on SMC

Table 3 gives the settings of design parameters Elbow-Exoskeleton System by SMC. The WOA algorithm was used to find the first set of design parameters, while the trial-and-error method was used to determine the second set. In order to provide the best possible control of the system, the optimum values of the design parameters determined via the WOA technique are transferred to the controllers' corresponding design parameters. The expected trajectory assumes a sine wave input.

**Table 3.** Setting of design parameters based on optimal and non-optimal methods

Controller	Optimal Method		Try and Error Method	
	Coefficient	Value	Coefficient	Value
SMC	$C$	78.8824	$C$	30
	$\beta_1$	561.14	$\beta_1$	500

### 6.2 Elbow-exoskeleton actuated system based on SMC

Figure 5 shows the linear position behaviour of the Elbow-Exoskeleton-actuated based on the optimal and non-optimal SMC to obtain the tracking performance for the system. It makes clear that the dynamic response obtained by the best SMC outperforms that based on the try-and-error process by a rate of about 45.5882% in terms of transient characteristics. The Figure 5 reflects the fact that the tracking error ( $e_1$ ) based on optimal is less than that due to non-optimal SMC, and thus optimal SMC gives better dynamic performance.

It is worth to mention that we have simulated optimized SMC parameter in which their error was 0.0111 compared whit 0.0204 for non-optimized SMC.

Figure 6 depicts the non-optimal SMC sliding surfaces, as well as the trace of the path in phase plane coordinates ( $e-e$ ). By the conclusion of the  $e$ -axis reaching phase, both trajectories had reached the sliding surface and stayed there until equilibrium was established.

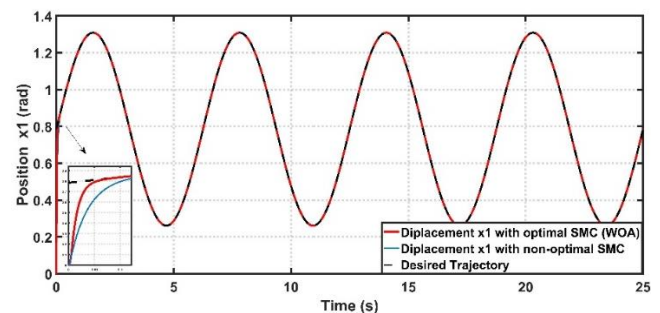


**Figure 5.** Tracking performance for the elbow-exoskeleton system with optimal and non-optimal SMC

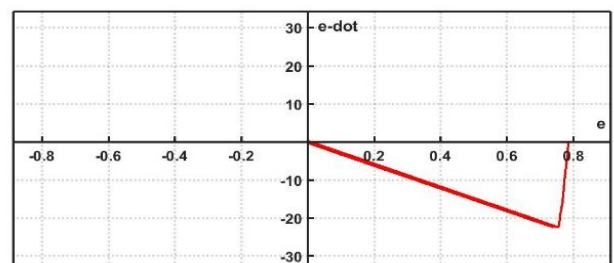


**Figure 6.** Sliding surface of non-optimal SMC

However, Figure 7 shows the tracking error of the elbow exoskeleton system controlled by optimal and non-optimal SMC (e). Again, the optimal SMC shows better performance in which covers wide range of torque. The effect of chattering phenomenon due to the SMC shows in Figure 8. Figure 9 explains the corresponding control effects based on optimal and non-optimal SMC.

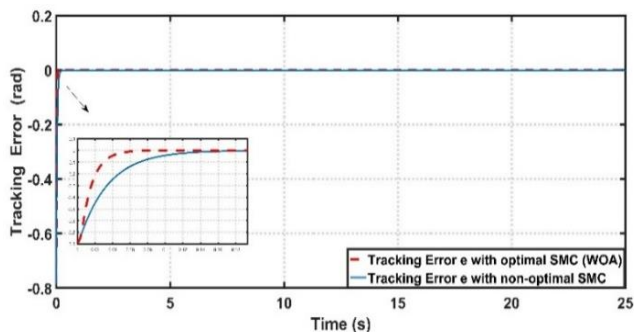


**Figure 7.** Tracking error of SMC controlled Elbow-Exoskeleton System

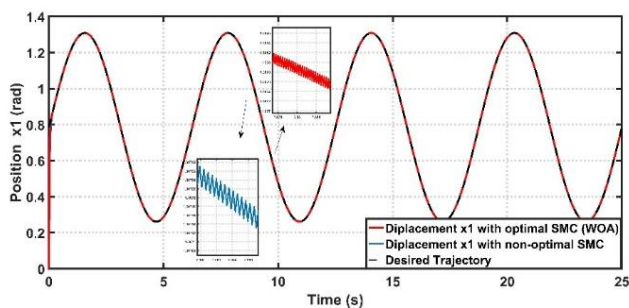


**Figure 8.** Chattering phenomenon based on SMC

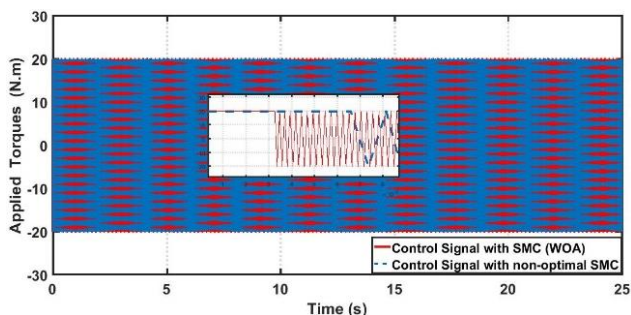


**Figure 9.** Control effects based on optimal and non-optimal SMC

## 7. CONCLUSIONS

In this study, control scheme have been designed for trajectory control tracking of elbow-assistive rehabilitation system. The control laws have been developed according to Lyapunov-based stability analysis. In comparison to previous studies, the design paramters of proposed controllers have been set based on try-and-error procedure. In this study, two settings of design parameters have been adopted. The classical setting is the first type of setting which is based on tray-and-error method, while the other setting is based on WOA. A comparison study in performance has been conducted to show the effectiveness of optimization method. The numerical results showed that the

WOA tuner could considerably enhanced the performance of proposed controllers. In addition, the dynamic performance of SMC-based Exoskeleton elbow system using WOA is better than that based on try-and-error procedure. This study can be extended to apply other recent control strategies for the elbow-exoskeleton system. Accordingly, one can conduct a comparison study between the SMC and the suggested control schemes to show their effectiveness in trajectory tracking [41-51].

## REFERENCES

- [1] Aljuboury, A.S., Hameed, A.H., Ajel, A.R., Humaidi, A.J., Alkhayyat, A., Mhdawi, A.K.A. (2022). Robust adaptive control of knee exoskeleton-assistant system based on nonlinear disturbance observer. *Actuators*, 11(3): 78. <https://doi.org/10.3390/act11030078>
- [2] Mahdi, S.M., Yousif, N.Q., Oglah, A.A., Sadiq, M.E., Humaidi, A.J., Azar, A.T. (2022). Adaptive synergetic motion control for wearable knee-assistive system: A rehabilitation of disabled patients. *Actuators*, 11(7): 176. <https://doi.org/10.3390/act11070176>
- [3] Alawad, N.A., Humaidi, A.J., Al-Araji, A.S. (2022). Improved active disturbance rejection control for the knee joint motion model. *Mathematical Modelling of Engineering Problems*, 9(2): 477-483. <https://doi.org/10.18280/mmep.090225>
- [4] Alawad, N.A., Humaidi, A.J., Al-Obaidi, A.S.M., Al-Araji, A.S. (2022). Active disturbance rejection control of wearable lower-limb system based on reduced ESO. *Indonesian Journal of Science & Technology*, 7(2): 203-218.
- [5] Alawad, N.A., Humaidi, A.J., Al-Araji, A.S. (2022). Observer sliding mode control design for lower exoskeleton system: Rehabilitation case. *Journal of Robotics and Control (JRC)*, 3(4): 476-482. <https://doi.org/10.18196/jrc.v3i4.15239>
- [6] Collinger, J.L., Foldes, S., Bruns, T.M., Wodlinger, B., Gaunt, R., Weber, D.J. (2013). Neuroprosthetic technology for individuals with spinal cord injury. *The Journal of Spinal Cord Medicine*, 36(4): 258-272. <https://doi.org/10.1179/2045772313Y.0000000128>
- [7] Nasiri, R., Shushtari, M., Arami, A. (2021). An adaptive assistance controller to optimize the exoskeleton contribution in rehabilitation. *Robotics*, 10(3): 95. <https://doi.org/10.3390/robotics10030095>
- [8] Hassan, M.Y., Karam, Z.A. (2015). Design and implementation of rehabilitation robot for human arm movements. *IJCCCE*, 15(2): 24-33.
- [9] Humaidi, A.J., Hasan, S., Al-Jodah, A.A. (2018). Design of second order sliding mode for glucose regulation systems with disturbance. *International Journal of Engineering and Technology (UAE)*, 7(2): 243-247. <http://dx.doi.org/10.14419/ijet.v7i2.28.12936>
- [10] Mohammad, A.M., AL-Samarraie, S.A. (2020). Robust controller design for flexible joint based on back-stepping approach. *Iraqi Journal of Computers, Communications, Control and Systems Engineering*, 20(2): 58-73. <http://dx.doi.org/10.33103/uot.ijccce.20.2.7>
- [11] Hameed, A.H., Al-Dujaili, A.Q., Humaidi, A.J., Hussein, H.A. (2019). Design of terminal sliding position control for electronic throttle valve system: A performance

- comparative study. *International Review of Automatic Control*, 12(5): 251-260. <https://doi.org/10.15866/ireaco.v12i5.16556>
- [12] Tohma, D.H., Hamoudi, A.K. (2021). Design of adaptive sliding mode controller for uncertain pendulum system. *Engineering and Technology Journal*, 39: 355-369. <https://doi.org/10.30684/etj.v39i3A.1546>
- [13] Al-Qassar, A.A., Abdulkareem, A.I., Hasan, A.F., Humaidi, A.J., Ibraheem, K.I., Azar, A.T., Hameed, A.H. (2021). Grey-wolf optimization better enhances the dynamic performance of roll motion for tail-sitter VTOL aircraft guided and controlled by STSMC. *Journal of Engineering Science and Technology*, 16(3): 1932-1950.
- [14] Adamiak, K. (2020). Chattering-free reference sliding variable-based SMC. *Mathematical Problems in Engineering*, 2020: 3454090. <https://doi.org/10.1155/2020/3454090>
- [15] Humaidi, A.J., Hameed, A.H. (2018). PMLSM position control based on continuous projection adaptive sliding mode controller. *Systems Science & Control Engineering*, 6(3): 242-252. <https://doi.org/10.1080/21642583.2018.1547887>
- [16] Humaidi, A.J., Hameed, A.H., Ibraheem, I.K. (2019). Design and performance study of two sliding mode backstepping control schemes for roll channel of delta wing aircraft. In 2019 6th International Conference on Control, Decision and Information Technologies (CoDIT), Paris, France, pp. 1215-1220. <https://doi.org/10.1109/CoDIT.2019.8820315>
- [17] Barbouch, H., Resquin, F., Gonzalez-Vargas, J., Hadded, N.K., Belghith, S. (2019). Feedback error learning with sliding mode control for functional electrical stimulation: Elbow joint simulation. *International Journal of Innovative Technology and Exploring Engineering (IJITEE)*, 8(12): 2971-2982. <https://doi.org/10.35940/ijitee.K2026.1081219>
- [18] Humaidi, A.J., Hameed, A.H. (2019). Design and comparative study of advanced adaptive control schemes for position control of electronic throttle valve. *Information*, (Switzerland), 10(2): 65. <https://doi.org/10.3390/info10020065>
- [19] Nguyen, H.T., Trinh, V.C., Le, T.D. (2020). An adaptive fast terminal sliding mode controller of exercise-assisted robotic arm for elbow joint rehabilitation featuring pneumatic artificial muscle actuator. *Actuators*, 9(4): 118. <https://doi.org/10.3390/act9040118>
- [20] Hu, B., Zhang, F., Lu, H., Zou, H., Yang, J., Yu, H. (2021). Design and assist-as-needed control of flexible elbow exoskeleton actuated by nonlinear series elastic cable driven mechanism. *Actuators*, 10(11): 290. <https://doi.org/10.3390/act10110290>
- [21] Brahmi, B., Rahman, M., Saad, M., Luna, C.O., Islam, M.R. (2016). Sliding mode-backstepping control for upper-limb rehabilitation with the ets-marse exoskeleton robot. RESNA: Arlington, VA, USA, pp. 1-7.
- [22] Liu, Y., Li, C., Teng, Z., Liu, K., Wang, G., Sun, Z. (2020). Intention recognition of elbow joint based on sEMG using adaptive fuzzy neural network. In 2020 5th International Conference on Mechanical, Control and Computer Engineering (ICMCCE), Harbin, China, pp. 1091-1096. <https://doi.org/10.1109/ICMCCE51767.2020.00240>
- [23] Yang, P., Sun, J., Wang, J., Zhang, G., Zhang, Y. (2019). Model-free based back-stepping sliding mode control for wearable exoskeletons. In 2019 25th International Conference on Automation and Computing (ICAC), pp. 1-6. <https://doi.org/10.23919/IconAC.2019.8895069>
- [24] Bembli, S., Haddad, N.K., Belghith, S. (2019). Adaptive sliding mode control with gravity compensation: Application to an upper-limb exoskeleton system. In MATEC Web of Conferences, 261: 06001. <https://doi.org/10.1051/matecconf/201926106001>
- [25] Islam, M.R., Rahmani, M., Rahman, M.H. (2020). A novel exoskeleton with fractional sliding mode control for upper limb rehabilitation. *Robotica*, 38(11): 2099-2120. <https://doi.org/10.1017/S0263574719001851>
- [26] Dinh, B.K., Xiloyannis, M., Antuvan, C.W., Cappello, L., Masia, L. (2017). Hierarchical cascade controller for assistance modulation in a soft wearable arm exoskeleton. *IEEE Robotics and Automation Letters*, 2(3): 1786-1793. <https://doi.org/10.1109/LRA.2017.2668473>
- [27] Sadiq, M.E., Humaidi, A.J., Kadhim, S.K., Mahdi, A.S., Alkhayyat, A., Ibraheem, I.K. (2021). Comparative study of optimal nonlinear control schemes for hanging mass actuated by uncertain pneumatic muscle. In 2021 IEEE 11th International Conference on System Engineering and Technology (ICSET), pp. 78-83. <https://doi.org/10.1109/ICSET53708.2021.9612530>
- [28] Sadiq, M.E., Humaidi, A.J., Kadhim, S.K., Al Mhdawi, A., Alkhayyat, A., Ibraheem, I.K. (2021). Optimal sliding mode control of single arm PAM-actuated manipulator. In 2021 IEEE 11th International Conference on System Engineering and Technology (ICSET), Shah Alam, Malaysia, pp. 84-89. <https://doi.org/10.1109/ICSET53708.2021.9612539>
- [29] Basri, M.A.M. (2018). Design and application of an adaptive backstepping sliding mode controller for a six-DOF quadrotor aerial robot. *Robotica*, 36(11): 1701-1727. <https://doi.org/10.1017/S0263574718000668>
- [30] Humaidi, A.J., Sadiq, M.E., Abdulkareem, A.I., Ibraheem, I.K., Azar, A.T. (2022). Adaptive backstepping sliding mode control design for vibration suppression of earth-quaked building supported by magneto-rheological damper. *Journal of Low Frequency Noise, Vibration and Active Control*, 41(2): 768-783. <https://doi.org/10.1177/14613484211064659>
- [31] Al-Qassar, A.A., Al-Obaidi, A.S.M., Hasan, A.F., Humaidi, A.J., Nasser, A.R., Alkhayyat, A., Ibraheem, I.K. (2021). Finite-time control of wing-rock motion for delta wing aircraft based on whale-optimization algorithm. *Indonesian Journal of Science and Technology*, 6(3): 441-456.
- [32] Mirjalili, S., Lewis, A. (2016). The whale optimization algorithm. *Advances in Engineering Software*, 95: 51-67. <https://doi.org/10.1016/j.advengsoft.2016.01.008>
- [33] Rana, N., Latiff, M.S.A., Abdulhamid, S.I.M., Chiroma, H. (2020). Whale optimization algorithm: A systematic review of contemporary applications, modifications and developments. *Neural Computing and Applications*, 32(20): 16245-16277. <https://doi.org/10.1007/s00521-020-04849-z>
- [34] Khadanga, R.K., Kumar, A., Panda, S. (2020). A novel modified whale optimization algorithm for load frequency controller design of a two-area power system composing of PV grid and thermal generator. *Neural Computing and Applications*, 32(12): 8205-8216. <https://doi.org/10.1007/s00521-019-04321-7>
- [35] Mosaad, A.M., Attia, M.A., Abdelaziz, A.Y. (2019).

- Whale optimization algorithm to tune PID and PIDA controllers on AVR system. *Ain Shams Engineering Journal*, 10(4): 755-767. <https://doi.org/10.1016/j.asej.2019.07.004>
- [36] Abdul-Kareem, A.I., Hasan, A.F., Al-Qassar, A.A., Humaidi, A.J., Hassan, R.F., Ibraheem, I.K., Azar, A.T. (2022). Rejection of wing-rock motion in delta wing aircrafts based on optimal LADRC schemes with butterfly optimization algorithm. *Journal of Engineering Science and Technology*, 17(4): 2476-2495.
- [37] Humaidi, A.J., Kadhim, S.K., Gataa, A.S. (2022). Optimal adaptive magnetic suspension control of rotary impeller for artificial heart pump. *Cybernetics and Systems*, 53(1): 141-167. <https://doi.org/10.1080/01969722.2021.2008686>
- [38] Ghanim, T., Ajel, A.R., Humaidi, A.J. (2020). Optimal fuzzy logic control for temperature control based on social spider optimization. *IOP Conference Series: Materials Science and Engineering*, 745(1): 012099. <https://iopscience.iop.org/article/10.1088/1757-899X/745/1/012099>.
- [39] Humaidi, A., Hameed, M. (2019). Development of a new adaptive backstepping control design for a non-strict and under-actuated system based on a PSO tuner. *Information (Switzerland)*, 10(2): 38. <https://doi.org/10.3390/info10020038>
- [40] Al-Azza, A.A., Al-Jodah, A.A., Harackiewicz, F.J. (2015). Spider monkey optimization: A novel technique for antenna optimization. *IEEE Antennas and Wireless Propagation Letters*, 15: 1016-1019. <https://doi.org/10.1109/LAWP.2015.2490103>.
- [41] Humaidi, A.J., Talaat, E.N., Hameed, M.R., Hameed, A.H. (2019). Design of adaptive observer-based backstepping control of cart-polependulum system. *Proceedings of 2019 3rd IEEE International Conference on Electrical, Computer and Communication Technologies, ICECCT 2019*. <http://dx.doi.org/10.1109/ICECCT.2019.8869179>
- [42] Hassan, M.Y., Humaidi, A.J., Hamza, M.K. (2020). On the design of backstepping controller for Acrobot system based on adaptive observer. *International Review of Electrical Engineering*, 15(4): 328-335. <https://doi.org/10.15866/iree.v15i4.17827>
- [43] Humaidi, A.J., Abdulkareem, A.I., Zhang, W. (2019). Design of augmented nonlinear PD controller of Delta/Par4 like robot. *Journal of Control Science and Engineering*, 2019(7): 1-11. <http://dx.doi.org/10.1155/2019/7689673>
- [44] Salman, M.A., Kadhim, S.K. (2022). Optimal backstepping controller design for prosthetic knee joint. *Journal Européen des Systèmes Automatisés*, 55(1): 49-59. <https://doi.org/10.18280/jesa.550105>
- [45] Humaidi, A.J., Hameed, M.R., Hameed, A.H. (2018). Design of block-backstepping controller to ball and arc system based on zero dynamic theory. *Journal of Engineering Science and Technology*, 13(7): 2084-2105.
- [46] Al-Shuka, H.F.N. (2020). Proxy-based sliding mode vibration control with an adaptive approximation compensator for euler-bernoulli smart beams. *Journal Européen des Systèmes Automatisés*, 53(6): 825-834. <https://doi.org/10.18280/jesa.530608>
- [47] Humaidi, A.J., Hameed, A.H., Hameed, M.R. (2018). Robust adaptive speed control for DC motor using novel weighted E-modified MRAC. *IEEE International Conference on Power, Control, Signals and Instrumentation Engineering, ICPCSI 2017*, pp. 313-319. <https://doi.org/10.1109/ICPCSI.2017.8392302>
- [48] Boudali, A., Negadi, K., Bouradi, S., Berkani, A., Marignetti, F. (2021). Design of nonlinear backstepping control strategy of PMSG for hydropower plant power generation. *Journal Européen des Systèmes Automatisés*, 54(1): 1-8. <http://dx.doi.org/10.18280/jesa.540101>
- [49] Humaidi, A.J., Hameed, A.H. (2017). Robustness enhancement of MRAC using modification techniques for speed control of three phase induction motor. *Journal of Electrical Systems*, 13(4): 723-741.
- [50] Euldji, R., Batel, N., Rebhi, R., Kaid, N., Tearnbucha, C., Sudsutad, W., Lorenzini, G., Ahmad, H., Ameer, H., Menni, Y. (2022). Optimal backstepping-FOPID controller design for wheeled mobile robot. *Journal Européen des Systèmes Automatisés*, 55(1): 97-107. <https://doi.org/10.18280/jesa.550110>
- [51] Humaidi, A.J., Hussein, H.A. (2019). Adaptive control of parallel manipulator in cartesian space. *2019 IEEE International Conference on Electrical, Computer and Communication Technologies (ICECCT), 2019*, pp. 1-8. <https://doi.org/10.1109/ICECCT.2019.8869257>

## NOMENCLATURE

$C$	Personal acceleration coefficient
$e$	Difference between the current position desired trajectory
$E_{ki}$	Kinetic energies
$E_{gi}$	Gravitational energies
$l$	Length
$L_i$	Elbow joint to center of gravity
$g$	Gravity Acceleration
$m_i$	Mass of the human elbow and exoskeleton
$k_i$	Viscous friction coefficients
$s$	Sliding surface
$w$	Inertia coefficient
$X_{1d}$	Desired trajectory

## Greek symbols

$\theta$	Angular position
$\dot{\theta}$	Angular velocity
$\ddot{\theta}$	Angular acceleration
$\tau_{exti}$	External torque
$\tau_{fi}$	Friction control torque
$\tau_g$	Gravitational torque
$\tau_i$	Motor control torque
$C$	Scalar design
$\beta_l$	Scalar design constant
$\alpha_l$	Virtual control

## Abbreviations

AFNN	Adaptive Fuzzy Neural Network
DoF	Degrees of freedoms
EES	Elbow Exoskeleton System
FL	Fuzzy Logic
FSMC	Fractional sliding mode control
RMSE	Root Mean Square Error
SMC	Sliding Mode Control